



**HAL**  
open science

**Synthesis, characterization and magnetic properties of  
four new organically templated metal sulfates  
[C<sub>5</sub>H<sub>14</sub>N<sub>2</sub>][M(II)(H<sub>2</sub>O)<sub>6</sub>](SO<sub>4</sub>)<sub>2</sub>, (M(II) = Mn, Fe, Co,  
Ni).**

Fadhel Hajlaoui, Houcine Naïli, Samia Yahyaoui, Mark M. Turnbull, Tahar  
Mhiri, Thierry Bataille

► **To cite this version:**

Fadhel Hajlaoui, Houcine Naïli, Samia Yahyaoui, Mark M. Turnbull, Tahar Mhiri, et al.. Synthesis, characterization and magnetic properties of four new organically templated metal sulfates [C<sub>5</sub>H<sub>14</sub>N<sub>2</sub>][M(II)(H<sub>2</sub>O)<sub>6</sub>](SO<sub>4</sub>)<sub>2</sub>, (M(II) = Mn, Fe, Co, Ni).. Dalton Transactions, 2011, 40 (43), pp.11613-20. 10.1039/c1dt11030f. hal-00824240

**HAL Id: hal-00824240**

**<https://hal.science/hal-00824240>**

Submitted on 21 May 2013

**HAL** is a multi-disciplinary open access archive for the deposit and dissemination of scientific research documents, whether they are published or not. The documents may come from teaching and research institutions in France or abroad, or from public or private research centers.

L'archive ouverte pluridisciplinaire **HAL**, est destinée au dépôt et à la diffusion de documents scientifiques de niveau recherche, publiés ou non, émanant des établissements d'enseignement et de recherche français ou étrangers, des laboratoires publics ou privés.

# Synthesis, characterization and magnetic properties of four new organically templated metal sulfates $[\text{C}_5\text{H}_{14}\text{N}_2][\text{M}^{\text{II}}(\text{H}_2\text{O})_6](\text{SO}_4)_2$ , ( $\text{M}^{\text{II}} = \text{Mn, Fe, Co, Ni}$ )<sup>†</sup>

Fadhel Hajlaoui,<sup>a</sup> Houcine Naili,<sup>\*a</sup> Samia Yahyaoui,<sup>a</sup> Mark M. Turnbull,<sup>b</sup> Tahar Mhiri<sup>a</sup> and Thierry Bataille<sup>c</sup>

Received 1st June 2011, Accepted 18th August 2011

DOI: 10.1039/c1dt11030f

A series of novel organically templated metal sulfates,  $[\text{C}_5\text{H}_{14}\text{N}_2][\text{M}^{\text{II}}(\text{H}_2\text{O})_6](\text{SO}_4)_2$  with ( $\text{M}^{\text{II}} = \text{Mn}$  (**1**),  $\text{Fe}$  (**2**),  $\text{Co}$  (**3**) and  $\text{Ni}$  (**4**)), have been successfully synthesized by slow evaporation and characterized by single-crystal X-ray diffraction as well as with infrared spectroscopy, thermogravimetric analysis and magnetic measurements. All compounds were prepared using a racemic source of the 2-methylpiperazine and they crystallized in the monoclinic systems,  $P2_1/n$  for (**1**, **3**) and  $P2_1/c$  for (**2**, **4**). Crystal data are as follows:  $[\text{C}_5\text{H}_{14}\text{N}_2][\text{Mn}(\text{H}_2\text{O})_6](\text{SO}_4)_2$ ,  $a = 6.6385(10)$  Å,  $b = 11.0448(2)$  Å,  $c = 12.6418(2)$  Å,  $\beta = 101.903(10)^\circ$ ,  $V = 906.98(3)$  Å<sup>3</sup>,  $Z = 2$ ;  $[\text{C}_5\text{H}_{14}\text{N}_2][\text{Fe}(\text{H}_2\text{O})_6](\text{SO}_4)_2$ ,  $a = 10.9273(2)$  Å,  $b = 7.8620(10)$  Å,  $c = 11.7845(3)$  Å,  $\beta = 116.733(10)^\circ$ ,  $V = 904.20(3)$  Å<sup>3</sup>,  $Z = 2$ ;  $[\text{C}_5\text{H}_{14}\text{N}_2][\text{Co}(\text{H}_2\text{O})_6](\text{SO}_4)_2$ ,  $a = 6.5710(2)$  Å,  $b = 10.9078(3)$  Å,  $c = 12.5518(3)$  Å,  $\beta = 101.547(2)^\circ$ ,  $V = 881.44(4)$  Å<sup>3</sup>,  $Z = 2$ ;  $[\text{C}_5\text{H}_{14}\text{N}_2][\text{Ni}(\text{H}_2\text{O})_6](\text{SO}_4)_2$ ,  $a = 10.8328(2)$  Å,  $b = 7.8443(10)$  Å,  $c = 11.6790(2)$  Å,  $\beta = 116.826(10)^\circ$ ,  $V = 885.63(2)$  Å<sup>3</sup>,  $Z = 2$ . The three-dimensional structure networks for these compounds consist of isolated  $[\text{M}^{\text{II}}(\text{H}_2\text{O})_6]^{2+}$  and  $[\text{C}_5\text{H}_{14}\text{N}_2]^{2+}$  cations and  $(\text{SO}_4)^{2-}$  anions linked by hydrogen-bonds only. The use of racemic 2-methylpiperazine results in crystallographic disorder of the amines and creation of inversion centers. The magnetic measurements indicate that the Mn complex (**1**) is paramagnetic, while compounds **2**, **3** and **4**, ( $\text{M}^{\text{II}} = \text{Fe, Co, Ni}$  respectively) exhibit single ion anisotropy.

## 1. Introduction

Over the past few decades, the chemistry of organically templated metal sulfates has been a rapidly expanding research field due to their fascinating structural diversities and potential applications as functional materials.<sup>1–14</sup> Particularly, the open-framework sulfates combining transition metal and organic groups are of great interest not only for their potential as model compounds of ferroelectric and ferroelastic domains, but also for their promising application in the field of molecular magnetism.<sup>15–16</sup> A variety of amines have been used previously in the preparation hybrid metal sulfates including aliphatic,<sup>15,17–18</sup> aromatic<sup>19–21</sup> and cyclic amines.<sup>3,7,22–26</sup> We have focused our attention on the study of a number of double

sulfates, combining transition metals with racemic amines containing N-donors such as 2-methylpiperazine. The use of transition metals in soft syntheses of sulfate-based compounds has provided supramolecular structures, related to that of the well-known Tutton's salts.<sup>27–29</sup> To improve the understanding of this type of hybrid material, a series of 3d transition metal sulfates templated by ( $\pm$ )-2-methylpiperazine,  $[\text{C}_5\text{H}_{14}\text{N}_2][\text{M}^{\text{II}}(\text{H}_2\text{O})_6](\text{SO}_4)_2$ , have been prepared. The use of the racemic mixture of the chiral amine in the reaction provides for alternatives in crystallization: a centrosymmetric structure where the enantiomers are related by an appropriate crystallographic symmetry operation, or one where the enantiomers occupy the same crystallographic position, generating disorder. The latter is the case in the present work, where we report the synthesis, crystal structure, thermal behaviour and magnetic properties of these compounds.

## 2. Experimental section

### 2.1. Materials

$\text{MnSO}_4 \cdot \text{H}_2\text{O}$  (99%, Merck),  $\text{FeSO}_4 \cdot 7\text{H}_2\text{O}$  (99%, Merck),  $\text{CoSO}_4 \cdot 7\text{H}_2\text{O}$  (99%, Merck),  $\text{NiSO}_4 \cdot 6\text{H}_2\text{O}$  (99%, Merck), 2-methylpiperazine (95%, Aldrich) and  $\text{H}_2\text{SO}_4$  (96%, Carlo Erba) were used as received. Distilled water was used in all syntheses.

<sup>a</sup>Laboratoire de l'Etat Solide, Département de Chimie, Université de Sfax, BP 1171, 3000 Sfax, Tunisia. E-mail: houcine\_naili@yahoo.com; Fax: (+216) 74 274 437; Tel: (+216) 98 66 00 26

<sup>b</sup>Carlson School of Chemistry and Biochemistry, Clark University, Worcester, MA, 01610, USA

<sup>c</sup>Sciences Chimiques de Rennes (UMR CNRS 6226), Groupe Matériaux Inorganiques: Chimie Douce et Réactivité, Université de Rennes I, Avenue du Général Leclerc, 35042, Rennes CEDEX, France

<sup>†</sup> Electronic supplementary information (ESI) available. Crystal data and structure refinement for compounds **1–4**, selected bond distances and angles for compounds **1–4** and selected bond distances and angles for  $[\text{SO}_4]$  tetrahedron in **1–4**. CCDC reference numbers 828000–828003. For ESI and crystallographic data in CIF or other electronic format see DOI: 10.1039/c1dt11030f

## 2.2. Synthesis

Compounds **1–4** were synthesized *via* slow evaporation from aqueous solution. The clear solutions were stirred for 15 min and allowed to stand at room temperature. After a few days, single crystals having the specified color (see below) were formed. The resulting mixtures were filtered, and the products washed with a small amount of cold distilled water and allowed to air dry. The yield was almost quantitative.

### [C<sub>5</sub>H<sub>14</sub>N<sub>2</sub>][Mn(H<sub>2</sub>O)<sub>6</sub>](SO<sub>4</sub>)<sub>2</sub> (**1**)

Compound **1** was synthesized through the reaction of 0.1690 g (1.00 × 10<sup>-3</sup> mol) of MnSO<sub>4</sub>·H<sub>2</sub>O, 0.1000 g (1.00 × 10<sup>-3</sup> mol) of 2-methylpiperazine, 0.1962 g (2.00 × 10<sup>-3</sup> mol) of H<sub>2</sub>SO<sub>4</sub>, and 4.9860 g (2.77 × 10<sup>-1</sup> mol) of water. White prismatic crystals were produced. IR data (cm<sup>-1</sup>): N–H 1515, 1591; C–H 3021; S–O 997, 1106; O–H 3435.

### [C<sub>5</sub>H<sub>14</sub>N<sub>2</sub>][Fe(H<sub>2</sub>O)<sub>6</sub>](SO<sub>4</sub>)<sub>2</sub> (**2**)

Compound **2** was synthesized through the reaction of 0.2779 g (1.00 × 10<sup>-3</sup> mol) of FeSO<sub>4</sub>·7H<sub>2</sub>O, 0.1000 g (1.00 × 10<sup>-3</sup> mol) of 2-methylpiperazine, 0.2128 g (2.17 × 10<sup>-3</sup> mol) of H<sub>2</sub>SO<sub>4</sub>, and 4.9500 g (2.75 × 10<sup>-1</sup> mol) of water. Dark green prismatic crystals were produced. IR data (cm<sup>-1</sup>): N–H 1463, 1634; C–H 3014; S–O 1094, 1195; O–H 3356.

### [C<sub>5</sub>H<sub>14</sub>N<sub>2</sub>][Co(H<sub>2</sub>O)<sub>6</sub>](SO<sub>4</sub>)<sub>2</sub> (**3**)

Compound **3** was synthesized through the reaction of 0.2811 g (1.00 × 10<sup>-3</sup> mol) of CoSO<sub>4</sub>·7H<sub>2</sub>O, 0.1000 g (1.00 × 10<sup>-3</sup> mol) of 2-methylpiperazine, 0.2168 g (2.21 × 10<sup>-3</sup> mol) of H<sub>2</sub>SO<sub>4</sub>, and 5.0040 g (2.78 × 10<sup>-1</sup> mol) of water. Red prismatic crystals were produced. IR data (cm<sup>-1</sup>): N–H 1508, 1495; C–H 3019; S–O 1090, 1186; O–H 3431.

### [C<sub>5</sub>H<sub>14</sub>N<sub>2</sub>][Ni(H<sub>2</sub>O)<sub>6</sub>](SO<sub>4</sub>)<sub>2</sub> (**4**)

Compound **4** was synthesized through the reaction of 0.2628 g (1.00 × 10<sup>-3</sup> mol) of NiSO<sub>4</sub>·6H<sub>2</sub>O, 0.1000 g (1.00 × 10<sup>-3</sup> mol) of 2-methylpiperazine, 0.2266 g (2.31 × 10<sup>-3</sup> mol) of H<sub>2</sub>SO<sub>4</sub>, and 4.9140 g (2.73 × 10<sup>-1</sup> mol) of water. Clear green prismatic crystals were produced. IR data (cm<sup>-1</sup>): N–H 1466, 1501; C–H 3012, S–O 1093, 1201; O–H 3411.

## 2.3. Single-crystal X-ray diffraction

Small crystals of the four compounds were glued to a glass fibre mounted on a four-circle Nonius Kappa CCD area-detector diffractometer. Intensity data sets were collected using Mo-K $\alpha$  radiation through the program COLLECT.<sup>30</sup> Corrections for Lorentz-polarisation effects, peak integration and background determination were carried out with the program DENZO.<sup>31</sup> Frame scaling and unit cell parameter refinements were performed with the program SCALEPACK.<sup>31</sup> Analytical absorption corrections were performed by modelling the crystal faces.<sup>32</sup> The structure analyses were carried out in the monoclinic space group *P*2<sub>1</sub>/*n* or *P*2<sub>1</sub>/*c*, according to the automated search for space groups available in Wingx.<sup>33</sup> Transition metal ions (M<sup>II</sup>) and sulfur atoms were located using the direct methods with program

SHELXS-97.<sup>34</sup> The oxygen atoms and the organic moieties were found from successive Fourier calculations using SHELXL-97.<sup>35</sup> The aqua H atoms were located in a difference map and refined with O–H distance restraints of 0.85(2) Å and H···H restraints of 1.39(2) Å so that the H–O–H angle fitted to the ideal value of a tetrahedral angle. H atoms bonded to C and N atoms were placed in geometrically idealized positions. Relevant crystallographic data are listed in Table 1, ESI.† Selected bond distances and angles are presented in Table 2 and 3, respectively, ESI.†

## 2.4. Infrared spectroscopy

Infrared measurements were obtained using a Perkin–Elmer FT-IR Spectrometer as KBr pellets in the range 4000–400 cm<sup>-1</sup>.

## 2.5. Thermogravimetric analysis

Thermogravimetric (TG) measurements were performed with a Rigaku Thermoflex instrument under flowing air for [C<sub>5</sub>H<sub>14</sub>N<sub>2</sub>][M<sup>II</sup>(H<sub>2</sub>O)<sub>6</sub>](SO<sub>4</sub>)<sub>2</sub> (M<sup>II</sup> = Mn (**1**), Fe (**2**), Co (**3**) and Ni (**4**)), in the temperature range 20–800 °C, with a heating rate of 5 °C min<sup>-1</sup>. The powdered samples (19.3 mg for **1**, 37.9 mg for **2**, 17.8 mg for **3** and 42.9 mg for **4**) were spread evenly in a large platinum crucible to avoid mass effects.

## 2.6. Powder X-ray diffraction

Temperature-dependent X-ray diffraction (TDXD), for compounds **1–4**, was performed with a D5005 powder diffractometer (Bruker AXS) using Cu-K $\alpha$  radiation [ $\lambda(K\alpha_1) = 1.5406$  Å,  $\lambda(K\alpha_2) = 1.5444$  Å] selected with a diffracted-beam graphite monochromator and equipped with an Anton Paar HTK1200 high-temperature oven camera. Powder X-ray diffraction was used to verify that materials used for magnetic and thermal analyses were the same phase as the single crystal structures for **1–4**. The thermal decomposition of compound **4** was carried out in air, with a heating rate of 7 °C h<sup>-1</sup> from ambient to 600 °C. Temperature calibration was carried out with standard materials in the involved temperature range. Experimental powder X-ray diffraction patterns at high temperature have been interpreted also by comparison with other compounds containing similar amine groups.<sup>5,6,7,37–38</sup>

## 2.7. Magnetic studies

Magnetic studies were performed on a Quantum Designs MPMS-XL SQUID magnetometer. Samples of each material were finely ground and packed in #4 gelatine capsules. The magnetic moment of the samples was then measured using a magnetic field varying from 0 to 50000 Oe at 1.8 K. Several data points were also collected as the field was reduced back to 0 to check for hysteresis effects; none were observed. For all samples, the moment was linear as a function of field to at least 4 kOe. The molar susceptibility  $\chi_M$ , defined as  $\chi_M = \lim_{B \rightarrow 0} (M_{\text{mol}}/B)$ , was collected as a function of temperature between 1.8 K and 310 K in a 1 kOe field.

## 3. Results

All of the hybrid compounds described within this work crystallize in the centrosymmetric space groups *P*2<sub>1</sub>/*n* and *P*2<sub>1</sub>/*c*. They consist of transition metal cations octahedrally coordinated by

six water molecules,  $[M^{II}(H_2O)_6]^{2+}$ , isolated sulfate anions  $(SO_4)^{2-}$  and disordered 2-methylpiperazinedium cations  $[C_5H_{14}N_2]^{2+}$ . The cohesion of these structures is ensured by hydrogen bonds between the cationic groups and the sulfate O atoms. The crystal structures of  $[C_5H_{14}N_2][M^{II}(H_2O)_6](SO_4)_2$  show similar coordination polyhedra. However, the arrangement of these polyhedra and the organic molecules varies slightly between complexes. We were able to distinguish two different structure types:  $[C_5H_{14}N_2][Mn(H_2O)_6](SO_4)_2$  and  $[C_5H_{14}N_2][Co(H_2O)_6](SO_4)_2$  (hence referred to as **1** and **3**, respectively) and  $[C_5H_{14}N_2][Fe(H_2O)_6](SO_4)_2$  and  $[C_5H_{14}N_2][Ni(H_2O)_6](SO_4)_2$  (hence referred to as **2** and **4**, respectively). The resulting H-bonding networks can be alternatively described by three-dimensional supramolecular frameworks belonging to two different structure types, forming channels in which the 2-methylpiperazinedium cations play a templating role. The packing for complexes **1** and **3** are depicted in Fig. 1a and 2, while that for complexes **2** and **4** are shown in Fig. 1b and 5.

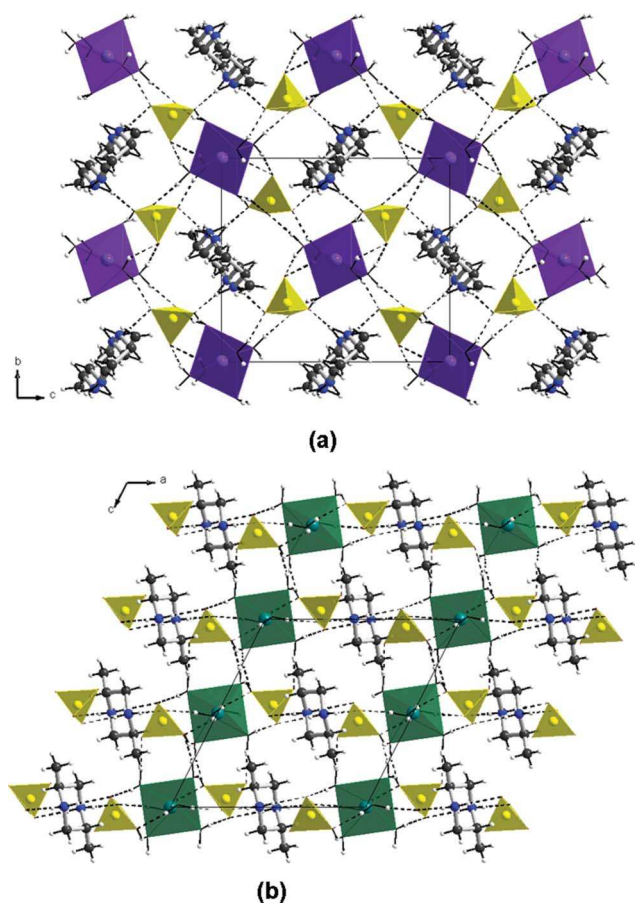


**Fig. 1** Three-dimensional packing in (a) **1** and (b) **2**. Selected hydrogen-bonding interactions are shown as dashed lines. Blue, green and yellow polyhedra represent  $[Mn(H_2O)_6]$ ,  $[Fe(H_2O)_6]$  and  $[SO_4]$ , respectively. Gray, blue, red and white spheres represent carbon, nitrogen, oxygen, and hydrogen, respectively.

Compounds **1** (Mn) and **3** (Co) are isostructural. The transition metal ions are located in special positions on crystallographic inversion centers and each is coordinated by six water-molecules oxygen atoms of which three are crystallographically independent. These  $[M^{II}(H_2O)_6]^{2+}$  octahedra are slightly distorted. The metal–oxygen distances vary from 2.1602(2) to 2.2013(2) Å for **1** and from

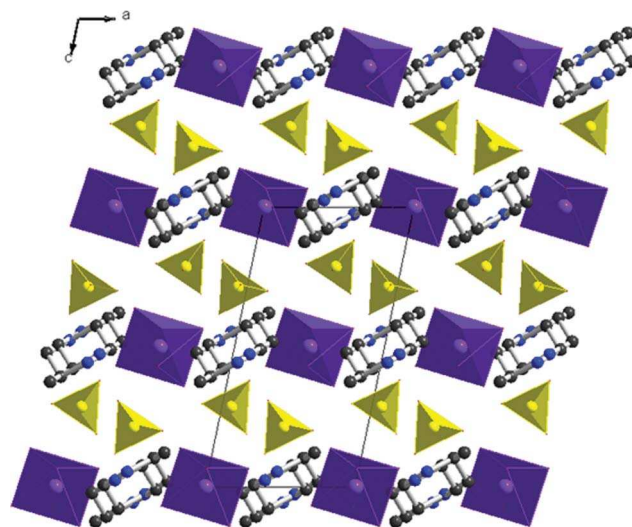


**Fig. 2** Projection of the extended structures of  $[C_5H_{14}N_2][Mn(H_2O)_6](SO_4)_2$  and  $[C_5H_{14}N_2][Co(H_2O)_6](SO_4)_2$ , along the *b*-axis. Blue and yellow polyhedra represent  $[Mn(H_2O)_6]$  or  $[Co(H_2O)_6]$  and  $[SO_4]$ , respectively. Gray, blue and red spheres represent carbon, nitrogen and oxygen, respectively. Hydrogen atoms have been removed for clarity.

2.0787(2) to 2.1105(2) Å for **3**. These values are in agreement with the values calculated from the bond valence program VALENCE<sup>36</sup> (2.174 Å and 2.113 Å in compounds **1** and **3**, respectively) for a six-fold oxygen-coordinated transition metal ion. Bond angles fall in the range 86.48(8)–93.52(8)° for O–Mn–O and 86.00(8)–94.00(8)° for O–Co–O, again analogous with other organically templated metal sulfates.<sup>3,7,16,37–40</sup> The  $M(O_w)_6$  octahedra are isolated from one to each other with a shortest distance Mn···Mn = 6.639(3) Å for (**1**) and Co···Co = 6.604(2) Å for (**3**), which are shorter than those found in related Mn and Co analogues.<sup>6,37,41</sup> The 2-methylpiperazinedium groups are located about crystallographic inversion centers, with all atoms located in general positions. In these two structures, a single disordered  $[C_5H_{14}N_2]^{2+}$  cation was observed with two orientations of both  $[R-C_5H_{14}N_2]^{2+}$  and  $[S-C_5H_{14}N_2]^{2+}$  enantiomers. The C and N atoms are distributed between two positions related by the symmetry center with a refined site occupancy factor equal to 0.5. For **1**, the N–C distances and the C–N–C angles range from 1.489(9) to 1.518(8) Å and from 113.0(6) to 113.6(6)°, while in **3**, the N–C distances vary from 1.479(10) to 1.507(2) Å and the C–N–C angles are in the range 112.2(7)–112.5(6)°. These values are in agreement with those found in related amine complexes.<sup>3,5,7,26</sup>

The  $[M(H_2O)_6]^{2+}$  cations occupy the corners and the center of the unit cell while the 2-methylpiperazinedium cations are located on the positions related by translation by 1/2 unit cell along the *b* and *c* axes, relative to the metal ions. Thus, the organic and inorganic cations alternate along the [010] and [001] directions and from mixed cationic layers perpendicular to the crystallographic *b* and *c* axes (see Fig. 1a and 2). The asymmetric unit of compounds **1** and **3** each contain only one independent regular  $SO_4$  tetrahedron. The sulfate ions are stacked such that they form anionic layers parallel to the cationic ones. The crystal structures are described by an alternation of cationic and anionic layers along [010] and [001]. The sulfate anions play an important role in the stability of the crystal structure by linking the organic and inorganic



cations *via* N–H...O and O<sub>w</sub>–H<sub>w</sub>...O hydrogen bonds. Indeed, all the O atoms of the sulfate anion participate as acceptors in hydrogen bonds (two from H-atoms bonded to N atoms and two from water H-atoms). These hydrogen bonds are fairly strong, with donor–acceptor distances range between 2.569(6) and 2.904(3) Å for **1** and between 2.566(6) and 2.943(3) Å for **3**. Each Mn<sup>II</sup>/Co<sup>II</sup> octahedron is surrounded by six sulfate groups H-bonded in a bidentate manner. Fig. 3 shows the neighbouring sulphate ions in the environment of the [M<sup>II</sup>(H<sub>2</sub>O)<sub>6</sub>] octahedron in [C<sub>5</sub>H<sub>14</sub>N<sub>2</sub>][M<sup>II</sup>(H<sub>2</sub>O)<sub>6</sub>](SO<sub>4</sub>)<sub>2</sub> with M<sup>II</sup> = Mn<sup>II</sup> or Co<sup>II</sup>.

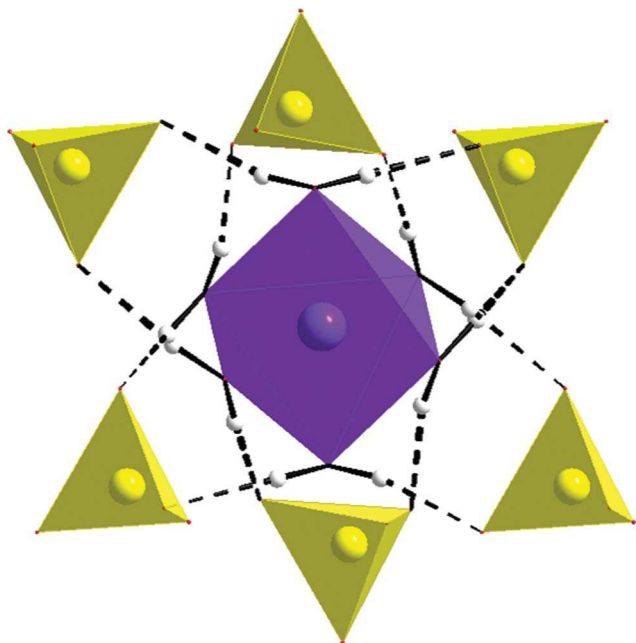


**Fig. 3** Neighbouring sulfates in the environment of [M<sup>II</sup>(H<sub>2</sub>O)<sub>6</sub>] in **1** and **3**. Blue and yellow polyhedra represent [Mn(H<sub>2</sub>O)<sub>6</sub>] or [Co(H<sub>2</sub>O)<sub>6</sub>] and [SO<sub>4</sub>], respectively.

The crystal structures of [C<sub>5</sub>H<sub>14</sub>N<sub>2</sub>][M<sup>II</sup>(H<sub>2</sub>O)<sub>6</sub>](SO<sub>4</sub>)<sub>2</sub> are similar to those of the manganese and cobalt templated by piperazine itself.<sup>37,41</sup> The only differences are observed in the direction of the charged-layers alternation and in the hydrogen bonds established between metal octahedra and sulfate tetrahedra.

In the crystal structures of **2** (Fe) and **4** (Ni), transition metal ions and disordered 2-methylpiperazinium cations are again located on crystallographic symmetry centers, while the sulfate tetrahedra lies in general positions. The supramolecular character of these phases is preserved, with the molecular arrangement of [C<sub>5</sub>H<sub>14</sub>N<sub>2</sub>][M<sup>II</sup>(H<sub>2</sub>O)<sub>6</sub>](SO<sub>4</sub>)<sub>2</sub> (M<sup>II</sup> = Fe, Ni) built from [M<sup>II</sup>(H<sub>2</sub>O)<sub>6</sub>]<sup>2+</sup>, (SO<sub>4</sub>)<sup>2-</sup> and disordered [C<sub>5</sub>H<sub>14</sub>N<sub>2</sub>]<sup>2+</sup> ions linked together by an extensive three-dimensional H-bonding network. The Fe<sup>2+</sup>/Ni<sup>2+</sup> cations are coordinated by six oxygen atoms forming a slightly distorted octahedra with the Fe–O distances in the range 2.1036(16)–2.1403(17) Å and the O–Fe–O angles in the range 86.59(7)–93.41(7)°, while the Ni–O distances range from 2.056(2) to 2.065(2) Å and O–Ni–O angles are between 85.98(9) and 94.02(9)°. These irregular octahedra are separated with a shortest Fe...Fe distance equal to 7.083(2) Å and a comparable Ni...Ni distance of 7.034(1) Å. These intermetallic distances are longer than that found in some analogous compounds.<sup>7,37–38</sup> This difference in the metal–metal distance is likely due to the size

and the shape of the amino groups involved in these structures. Bond valences were calculated for compounds **2** and **4**, in which the values of the Fe<sup>2+</sup> and Ni<sup>2+</sup> centers are equal to 2.131 Å and 2.043 Å, respectively. The Fe<sup>2+</sup>/Ni<sup>2+</sup> octahedra are linked together by O<sub>w</sub>–H<sub>w</sub>...O hydrogen bonds through the sulfate tetrahedra. Fig. 4 shows how each [M<sup>II</sup>(H<sub>2</sub>O)<sub>6</sub>]<sup>2+</sup> unit is connected to two SO<sub>4</sub><sup>2-</sup> anions in a tridentate manner, two sulfate groups in a bidentate manner and two sulfate groups in a monodentate fashion. In compound **2**, the organic cations become partially disordered with C–C and N–C distances ranging from 1.294(6) to 1.516(4) Å and from 1.469(5) to 1.498(4) Å, respectively. The C–N–C angles are equal to 111.8(2)°. Similarly, the C–C and N–C bonds in **4** range between 1.298(8) and 1.517(5) Å, 1.471(6) and 1.504(5) Å, respectively. The C–N–C angles are the same as those in **2** within experimental error. These values, in agreement with those found in the Fe and Ni complexes templated by dabco,<sup>37–38</sup> deviate somewhat from others found in the literature.<sup>42</sup> This deviation seems to be a consequence of the disordered methyl groups in the organic cations. The disordered [C<sub>5</sub>H<sub>14</sub>N<sub>2</sub>]<sup>2+</sup> cations reside between the inorganic layers, balancing charge and participating in the extensive hydrogen-bonding network.

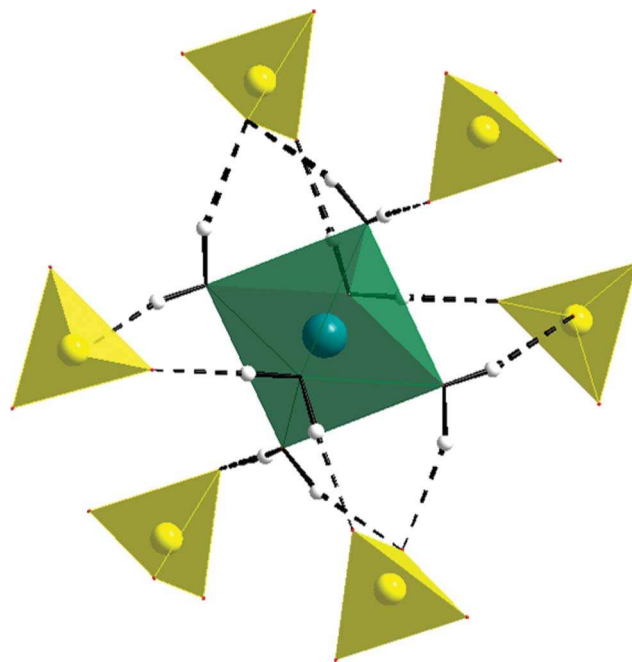


**Fig. 4** Neighbouring sulfates in the environment of [M<sup>II</sup>(H<sub>2</sub>O)] in **2** and **4**. Green and yellow polyhedra represent [Fe(H<sub>2</sub>O)<sub>6</sub>] or [Ni(H<sub>2</sub>O)<sub>6</sub>] and [SO<sub>4</sub>], respectively.

As seen in Fig. 1b, the structures of **2** and **4** can also be described as an alternation between organic and inorganic layers along the *a*-axis. On the other hand, the organic and inorganic cations also alternate along the [101] direction so that they form mixed cationic layers parallel to *b*-axis (see Fig. 5).

The structures of compounds **2** and **4** are closely related. Each asymmetric unit contains only one sulfur atom located on a general position and tetrahedrally coordinated by four oxygen atoms. These anions link the organic and inorganic cations by two types of hydrogen bonds: O<sub>w</sub>–H<sub>w</sub>...O and N–H...O. Within the intermolecular bonds, the N...O distances vary between 2.767(3)

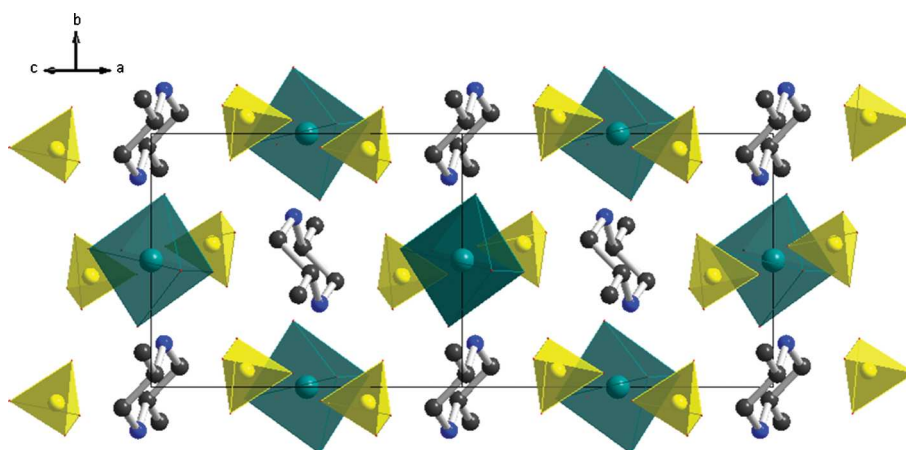


**Fig. 5** View of extended structures of **2** and **4** down the crystallographic [101] axis. Green and yellow polyhedra represent  $[\text{Fe}(\text{H}_2\text{O})_6]$  or  $[\text{Ni}(\text{H}_2\text{O})_6]$  and  $[\text{SO}_4]$ , respectively. Gray, blue and red spheres represent carbon, nitrogen and oxygen, respectively. Hydrogen atoms have been removed for clarity.

and 2.866(3) Å in **2** and between 2.763(4) and 2.871(4) Å in **4**. The  $\text{O}_w \cdots \text{O}$  distances range from 2.694(3) to 2.810(2) Å and between 2.700(3) and 2.805(3) Å in **2** and **4**, respectively.

#### 4. Thermal decomposition

The thermogravimetric analysis (TG) curves obtained during the decomposition of compounds **1–4**, under flowing air are shown in Fig. 6. This demonstrates that the decomposition of the compounds is complex and takes place through several stages.

Compound **1** (Mn). Fig. 6a shows the TG curve obtained during the decomposition of  $[\text{C}_5\text{H}_{14}\text{N}_2][\text{Mn}(\text{H}_2\text{O})_6](\text{SO}_4)_2$  in the temperature range 20–800 °C. The first weight loss (7.51%), observed between room temperature and 125 °C, is attributed to the departure of two water molecules (calculated weight loss, 7.87%). The second weight loss, observed between 127 and 191 °C, is attributed to departure of the remaining water molecules to form the anhydrous compound  $[\text{C}_5\text{H}_{14}\text{N}_2]\text{Mn}(\text{SO}_4)_2$ . The amine decomposition together with one sulfate group gives rise to the  $\beta$  variety of manganese sulfate at  $\sim 457.27$  °C (observed weight loss, 42.52%, theoretical, 43.34%). The last step takes place between 534 and 794 °C and corresponds to the decomposition of  $\beta$ - $\text{MnSO}_4$  into  $\text{Mn}_2\text{O}_3$ .<sup>6</sup>

Compound **2** (Fe). The TG curve, carried out between 20 and 800 °C, is shown in Fig. 6b and exhibits five successive weight losses. The first transformation occurs over the temperature range 25–160 °C and the weight loss of 11.83% is in agreement with the departure of three water molecules (calculated weight loss, 11.78%). The second weight loss of 13.97%, observed between 160–209 °C, corresponds to the departure of the last three water molecules (calculated weight loss, 13.35%), leading to the anhydrous phase  $[\text{C}_5\text{H}_{14}\text{N}_2]\text{Fe}(\text{SO}_4)_2$ . The decomposition of the anhydrous phase starts near 230 °C, includes loss of the organic moiety, and leads to  $\text{Fe}_2(\text{SO}_4)_3$ . This result is evidenced by the weight loss of 51.34% (calculated weight loss, 51.2%). The subsequent decomposition of  $\text{Fe}_2(\text{SO}_4)_3$  between 518 and 680 °C is in agreement with the global formula  $\text{Fe}_2\text{O}_2(\text{SO}_4)$ . The final stage corresponds to the decomposition of the iron sulfate into  $\text{Fe}_2\text{O}_3$ .<sup>37</sup>

Compound **3** (Co). Decomposition of  $[\text{C}_5\text{H}_{14}\text{N}_2][\text{Co}(\text{H}_2\text{O})_6](\text{SO}_4)_2$  between 20 and 800 °C, proceeds through

four main stages (see Fig. 6c). Five water molecules are lost over the temperature range 25–168 °C (observed weight loss, 20.01%, theoretical, 19.50%). The second stage, near 170 °C, coincides with loss of the remaining water molecule to form the anhydrous compound  $[\text{C}_5\text{H}_{14}\text{N}_2]\text{Co}(\text{SO}_4)_2$  (observed weight loss, 4.12%, theoretical, 3.90%). The anhydrous phase is stable to 341 °C and then transforms into the  $\beta$ -phase of cobalt sulfate (observed weight loss, 55.82%; theoretical, 56.12%). The last stage, beginning near 547°, corresponds to the decomposition of the cobalt sulfate, giving rise to the mixed cobalt oxide  $\text{Co}_3\text{O}_4$ .<sup>15</sup>

Compound **4** (Ni). The data are shown in Fig. 6d. Four successive weight losses are observed. Dehydration of the precursor occurs in two stages. First, a weight loss of 4.32% observed at 180 °C corresponds to the departure of a single water molecule (theoretical weight loss, 3.90%). The second stage of the dehydration takes place between 190 and 300 °C, and correspond to the departure of the remaining water molecules (observed weight loss, 20.43%; calculated weight loss, 20.31%). Fig. 6e shows the three-dimensional representation of the powder diffraction patterns obtained during the decomposition of  $[\text{C}_5\text{H}_{14}\text{N}_2][\text{Ni}(\text{H}_2\text{O})_6](\text{SO}_4)_2$  under flowing air in the temperature 20–600 °C. This plot reveals that the precursor is stable until 130 °C and then transforms into the anhydrous phase,  $[\text{C}_5\text{H}_{14}\text{N}_2]\text{Ni}(\text{SO}_4)_2$ , amorphous (am.) to X-rays. The anhydrous compound observed on the TG curve, is stable between 225 °C and 300 °C. The next transformation starts at  $\sim 310$  °C and corresponds to the decomposition of the amine entity and partial decomposition of the sulfate groups.  $\text{NiSO}_4$  is formed at 430 °C, and starts to decompose into  $\text{NiO}$  at 565 °C. Consequently, the given product is a mixture of crystallized  $\text{NiSO}_4$  (PDF N° 01-076-0220) and  $\text{NiO}$  (PDF N° 00-044-1159) phases, as also confirmed by the TDXD plot at 582 °C. This result is not surprising as it has already been observed in the piperazine<sup>37</sup> and dabco<sup>38</sup> related compounds. The end of the decomposition corresponds to the total decomposition of the  $\text{NiSO}_4$  into  $\text{NiO}$  at 760 °C.

#### 5. Magnetic properties

The temperature dependence of the magnetic susceptibility for compounds **1–4** was determined over the range 1.8–310 K in a 0.1 T field and the results are shown in Fig. 7 and 8. The Mn

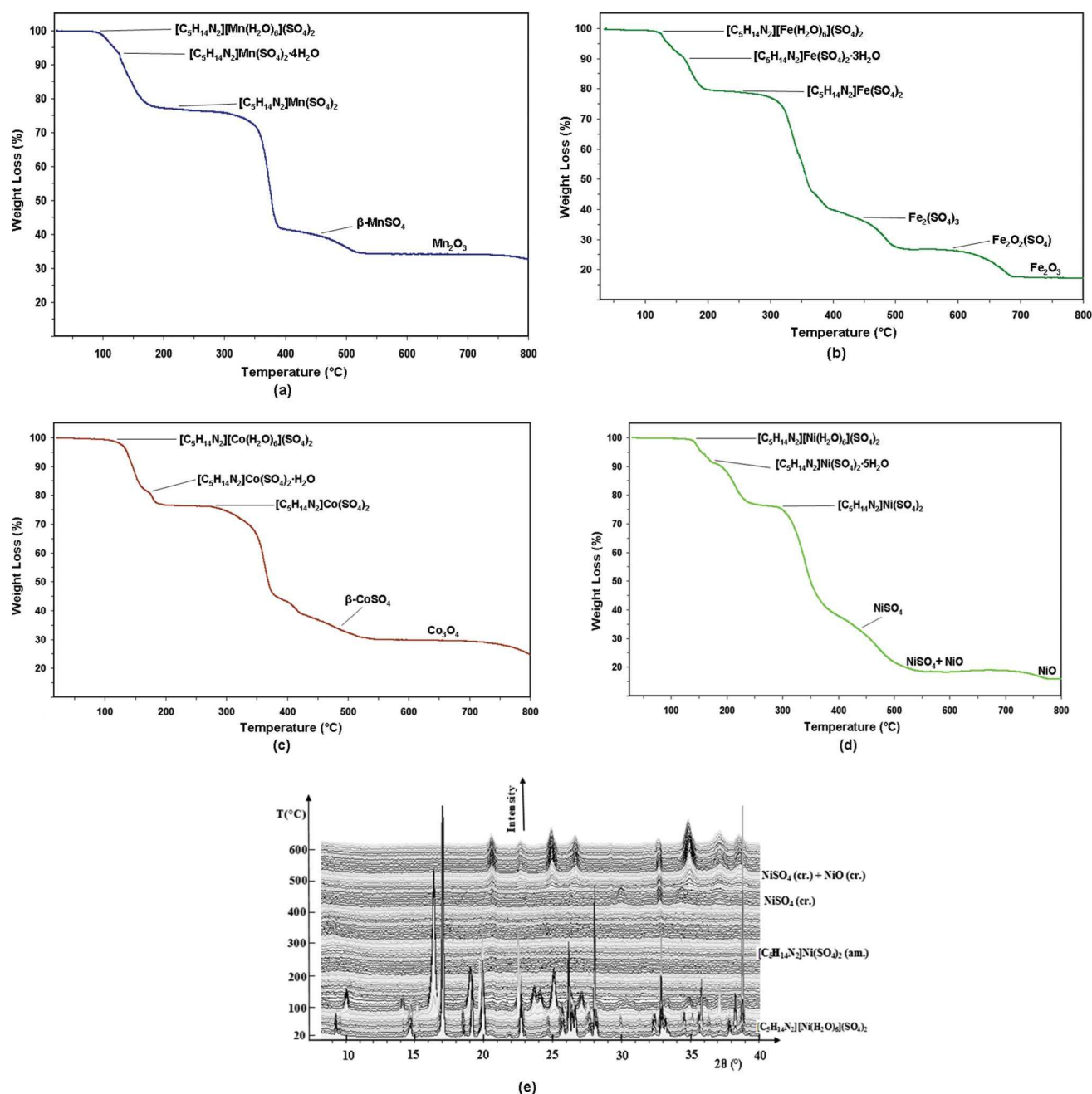


**Fig. 6** Thermogravimetric analysis for compounds (a) **1**, (b) **2**, (c) **3** and (d) **4**. The TDXD plot for the decomposition of  $[\text{C}_5\text{H}_{14}\text{N}_2][\text{Ni}(\text{H}_2\text{O})_6](\text{SO}_4)_2$  is shown in figure (e) **4**.

complex, **1**, shows typical paramagnetic behavior with a Curie constant ( $C$ ) of 4.46(2) and a Curie–Weiss  $\theta = 0.07(10)$ , typical of an Mn(II) complex with negligible interactions (Fig. 7).<sup>43</sup> The magnetic susceptibility values of **2** (the Fe(II) complex) follows a Curie–Weiss law from room temperature to below 50 (Fig. 8a) with values for  $C$  and  $\theta$  equal to 3.5(1) emu·K mol<sup>-1</sup>, typical of Fe(II) complexes<sup>43–46</sup> and 0.7(5) K, respectively, suggesting negligible interactions. Below 50 K, the value of  $\chi_m^*T$  begins to decrease significantly, eventually reaching 0.84 at 1.8 K. Fitting of the data to a single ion anisotropy model using MAGMUN<sup>47</sup> gave a value of  $D = -11(1)$  and  $g = 2.16(2)$  with a Curie–Weiss correction of  $-0.2$ , as expected of isolated octahedral Fe(II) complexes.<sup>48</sup> The

cobalt complex, **3**, behaves similarly (Fig. 8b). The  $\chi_m^*T$  product decreases at low temperatures, approaching a value of 1.7 as  $T$  approaches zero, again in agreement with single ion anisotropy.<sup>48</sup> The data were fit to a single ion anisotropy model which gave a Curie constant of 3.03(6) and  $D = -52(4)$ . A fit to the same model including a Curie–Weiss correction gave identical results for  $C$  and  $D$  within error, and a Weiss correction of  $-0.1(2)$  supporting the weakness of the exchange interactions. Finally, fitting of the data for the Ni(II) complex **4** (Fig. 8c) resulted in a Curie constant of 1.24(1) and a  $D$  value of  $-3.58(7)$ , in good agreement with expected values.<sup>43,48</sup> The Curie–Weiss plot gave a  $\theta = 0.4(2)$ , again in agreement with negligible intermolecular exchange.

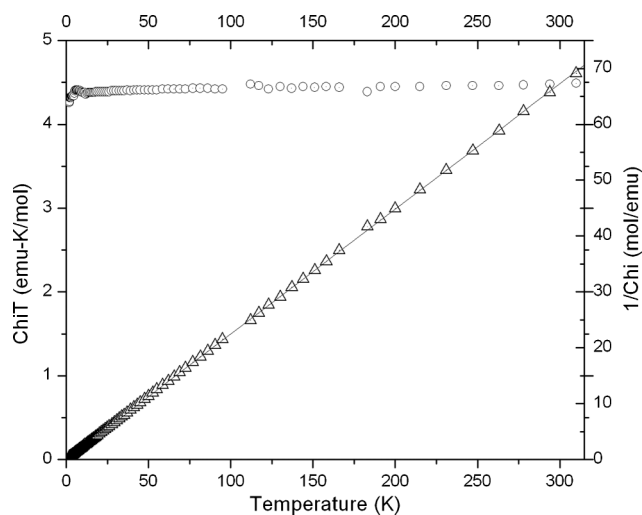


**Fig. 7** Thermal dependence of the  $\chi_m T$  product (open circles) and  $1/\chi_m$  as a function of temperature for compound **1**.

## 6. Discussion

Compounds **1–4** all crystallize in centrosymmetric space groups. The use of racemic 2-methylpiperazine in each system tends to direct crystallization toward centric space groups (although this is not required). The result that the enantiomeric organic cations in the structures are crystallographically disordered, rather than symmetry related, suggests that there was sufficient void volume in the structure to accommodate the disorder (the volume required for the disordered cations is somewhat larger than that required for either enantiomer). The fact that the disorder occurs in spite of an extensive hydrogen-bonding network is readily explained by the observation that the methylpiperazinediium cations in both positions are hydrogen bonded to water molecules, negating any possible thermodynamic preference for one or the other. The use of a rigid diamine can deter orientational disorder within the organic amine, through the combination of low molecular flexibility and multiple points of interaction between the amine and inorganic components. Despite this, two disorder mechanisms are observed in these complexes for the  $[\text{C}_5\text{H}_{14}\text{N}_2]^{2+}$  cations. Inversion symmetry within the cations results in the superimposition of both  $[\text{R}-\text{C}_4\text{H}_{12}\text{N}_2]^{2+}$  and  $[\text{S}-\text{C}_4\text{H}_{12}\text{N}_2]^{2+}$  (see Fig. 9). Such disorders are founded in the related gallium fluorophosphates.<sup>26</sup>

Counterpoints to the role of template disorder in these compounds can be found in related systems based upon the templated copper sulfate compound,  $[\text{C}_5\text{H}_{14}\text{N}_2][\text{Cu}(\text{H}_2\text{O})_6(\text{SO}_4)] \cdot \text{H}_2\text{O}^3$  which was synthesized using the same amine under slow evaporation conditions and crystallized in the centrosymmetric space group  $P2_1/n$ . Both  $[\text{R}-\text{C}_5\text{H}_{14}\text{N}_2]^{2+}$  and  $[\text{S}-\text{C}_5\text{H}_{14}\text{N}_2]^{2+}$  cations were generated *via* inversion from a single ordered  $[\text{C}_5\text{H}_{14}\text{N}_2]^{2+}$  cation in the asymmetric unit.

The structural aspects of **1–4** are reminiscent of another group of compounds with the formula  $\text{A}_2\text{M}(\text{H}_2\text{O})_6(\text{XO}_4)_2$  ( $\text{A}$  = monovalent cation,  $\text{M}$  = divalent cation,  $\text{X}$  = hexavalent cation), popularly referred to as Tutton's salts. It is surprising since there is no relation between the decrease of ionic radius of the cation from  $\text{Mn}^{2+}$  to  $\text{Ni}^{2+}$  and the structural arrangement observed for these supramolecular sulfates. On the contrary, the use of  $\text{NH}_4^+$  instead 2-methylpiperazinediium with all transition metal sulfates gives

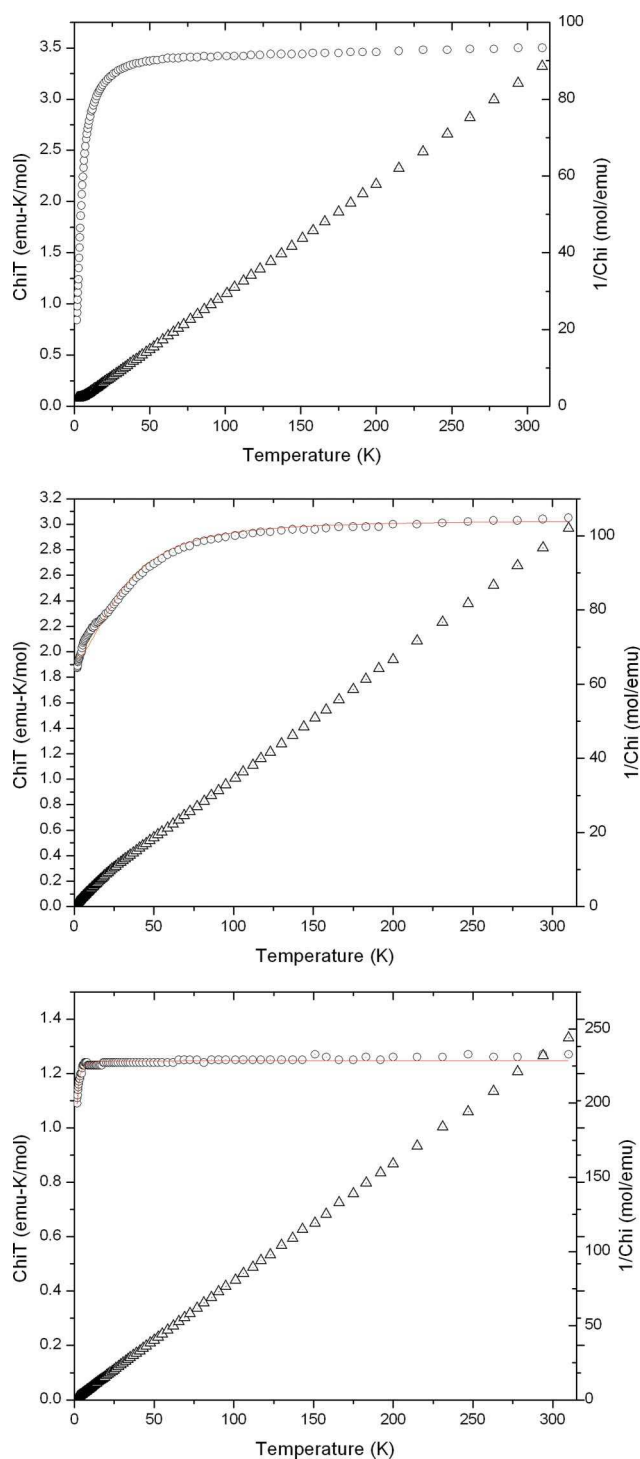


**Fig. 8** Thermal dependence of the  $\chi_m T$  product (open circles) and  $1/\chi_m$  as a function of temperature for compounds (a) **2**, (b) **3**, and (c) **4**. For **8b** and **8c**, the solid line shows the fit to a single ion anisotropy model.

rise to the isostructural Tutton's salts structure.<sup>27–29</sup> Further studies to understand the templating role of diamines in the presence of transition metal sulfates are under way. The thermogravimetric analysis (TGA) curves for compounds **1–4** show that there are similar changes in the decompositions of precursors with somewhat smaller differences, which could be associated with the structural variations. The first noticeable point is related to the



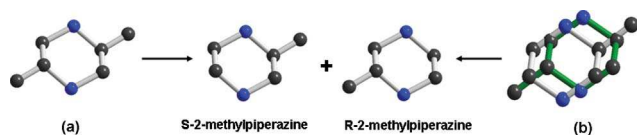


**Fig. 9** Disorder mechanism present in the  $[C_5H_{14}N_2]^{2+}$  cations for the (a) in (2, 4) and for (b) in (1, 3). Gray and blue spheres represent carbon and nitrogen, respectively. Hydrogen atoms have been removed for clarity.

difference of the dehydration temperatures that could be explained by the nature of the metal as well as the hydrogen bonds involved in the structures.

## Concluding remarks

Four new organically templated complexes with the formula  $[C_5H_{14}N_2][M^{II}(H_2O)_6](SO_4)_2$  have been prepared by slow evaporation. The structures consist of isolated  $M^{II}$  ions ( $M = Mn, Fe, Co, Ni$ ) octahedrally coordinated by six water molecules, diprotonated 2-methylpiperazinedium cations and sulfate anions linked by hydrogen bonds. Two structure types were distinguished and described. The centrosymmetric crystal structures of the title compounds were expected from the racemic character of the amine used in these syntheses. The thermal behaviour of the precursors is shown to be dependent not only on the structure type but also on the transition metal atom involved in the structure. Magnetic measurements revealed the presence of single ion anisotropy for compounds 2–4. This work contributes to the research on the sulfate chemistry based organic–inorganic hybrids complex with novel topologies and interesting magnetic properties.

## Acknowledgements

Grateful thanks are expressed to Dr T. Roisnel (Centre de Diffraction X, Université de Rennes I) for the assistance with single-crystal X-ray diffraction data collection.

## References

- 1 C. N. R. Rao, J. N. Behera and M. Dan, *Chem. Soc. Rev.*, 2006, **35**, 375.
- 2 M. B. Doran, A. J. Norquist and D. O'Hare, *Inorg. Chem.*, 2003, **42**, 6989.
- 3 F. Hajlaoui, S. Yahyaoui, H. Naïli, T. Mhiri and T. Bataille, *Polyhedron*, 2009, **28**, 2113.
- 4 F. Hajlaoui, S. Yahyaoui, H. Naïli, T. Mhiri and T. Bataille, *Inorg. Chim. Acta*, 2010, **363**, 691.
- 5 W. Rekik, H. Naïli, T. Mhiri and T. Bataille, *Solid State Sci.*, 2009, **11**, 614.
- 6 W. Rekik, H. Naïli, T. Mhiri and T. Bataille, *J. Chem. Crystallogr.*, 2007, **37**, 147.
- 7 S. Yahyaoui, W. Rekik, H. Naïli, T. Mhiri and T. Bataille, *J. Solid State Chem.*, 2007, **180**, 3560.
- 8 Y.-P. Yuan, R.-Y. Wang, D.-Y. Kong, J.-G. Mao and A. Clearfield, *J. Solid State Chem.*, 2005, **178**, 2030.
- 9 Y. Xu, S. Ding and X. Zheng, *J. Solid State Chem.*, 2007, **180**, 2020.
- 10 R. E. Wilson, S. Skanthakumar, K. E. Knope, C. L. Cahill and L. Soderholm, *Inorg. Chem.*, 2008, **47**, 9321.
- 11 T. Bataille and D. Louer, *J. Solid State Chem.*, 2004, **177**, 1235.

- 12 J. N. Behera, K. V. Gopalkrishnan and C. N. R. Rao, *Inorg. Chem.*, 2004, **43**, 2636.
- 13 I. Bull, P. S. Wheatley, P. Lightfoot, R. E. Morris, E. Sastre and P. A. Wright, *Chem. Commun.*, 2002, 1180.
- 14 P. S. Halasyamani and A. J. Norquist, *Cryst. Growth Des.*, 2005, **5**, 1913.
- 15 W. Rekik, H. Naïli, T. Mhiri and T. Bataille, *Mater. Res. Bull.*, 2008, **43**, 2709.
- 16 J. N. Bahera and C. N. R. Rao, *Chem.–Asian J.*, 2006, **1**, 742.
- 17 E. A. Kaufman, M. Zeller and A. J. Norquist, *Cryst. Growth Des.*, 2010, **10**, 4656.
- 18 A. J. Norquist, M. B. Doran and D. O'Hare, *Inorg. Chem.*, 2005, **44**, 3837.
- 19 C. Y. Chen, K. H. Lii and A. J. Jacobson, *J. Solid State Chem.*, 2003, **172**, 252.
- 20 X. Y. Wang, H. Y. Wei, Z. M. Wang, Z. D. Chen and S. Gao, *Inorg. Chem.*, 2005, **44**, 572.
- 21 Y. Li, J. Lü and R. Cao, *Inorg. Chem. Commun.*, 2009, **12**, 181.
- 22 E. A. Muller, R. J. Cannon, A. N. Sarjeant, K. M. Ok, P. S. Halasyamani and A. J. Norquist, *Cryst. Growth Des.*, 2005, **5**, 1913.
- 23 H. S. Casalongue, S. J. Choyke, A. N. Sarjeant, J. Schrier and A. J. Norquist, *J. Solid State Chem.*, 2009, **182**, 1297.
- 24 W. Rekik, H. Naïli, T. Mhiri and T. Bataille, *Acta Crystallogr., Sect. E: Struct. Rep. Online*, 2009, **E65**, 1404.
- 25 A. J. Norquist, P. M. Thomas, M. B. Doran and D. O'Hare, *Chem. Mater.*, 2002, **14**, 5179.
- 26 S. J. Choyke, S. M. Blau, A. A. Larner, A. N. Sarjeant, J. Yeon, P. S. Halasyamani and A. J. Norquist, *Inorg. Chem.*, 2009, **48**, 11277.
- 27 V. Koleva and D. Stoilova, *Thermochim. Acta*, 1999, **342**, 89.
- 28 H. Montgomery, R. V. Chastain and E. C. Lingafelter, *Acta Crystallogr.*, 1966, **20**, 731.
- 29 H. Montgomery, R. V. Chastain, J. J. Natt, A. M. Witkowska and E. C. Lingafelter, *Acta Crystallogr.*, 1967, **22**, 775.
- 30 Nonius, Kappa CCD Program Software, Nonius BV, Delft, the Netherlands, 1998.
- 31 Z. Otwinowski, W. Minor, C. W. Carter and R. M. Sweet, *Methods in Enzymology*, **276**, Academic Press, New York, 1997, 307.
- 32 J. De Meulenaer and H. Tompa, *Acta Crystallogr.*, 1965, **19**, 1014.
- 33 L. J. Farrugia, *J. Appl. Crystallogr.*, 1999, **32**, 837.
- 34 G. M. Sheldrick, *SHELXS-97*, Programs for Crystal Structure Solution, University of Gottingen, Germany, 1997.
- 35 G. M. Sheldrick, *SHELXL-97*, Programs for Crystal Structure Refinement, University of Gottingen, Germany, 1997.
- 36 I. D. Brown, *J. Appl. Crystallogr.*, 1996, **29**, 479.
- 37 W. Rekik, H. Naïli, T. Bataille, T. Roisnel and T. Mhiri, *Inorg. Chim. Acta*, 2006, **359**, 3954.
- 38 W. Rekik, H. Naïli, T. Bataille and T. Mhiri, *J. Organomet. Chem.*, 2006, **691**, 4725.
- 39 H. Naïli, W. Rekik, T. Bataille and T. Mhiri, *Polyhedron*, 2006, **25**, 3543.
- 40 Y. Xing, Y. Liu, Z. Shi, H. Meng and W. Pang, *J. Solid State Chem.*, 2003, **174**, 381.
- 41 J.-X. Pan, G.-Y. Yang and Y.-Q. Sun, *Acta Crystallogr., Sect. E: Struct. Rep. Online*, 2003, **E59**, 286.
- 42 K. Jayaraman, A. Choudhury and C. N. R. Rao, *Solid State Sci.*, 2002, **4**, 413.
- 43 R. L. Carlin, *Magneto-chemistry* Springer-Verlag, New York, 1986.
- 44 F. Sanz, C. Parada, J. M. Rojo and C. Ruiz-Valero, *Chem. Mater.*, 2001, **13**, 1334.
- 45 C. N. R. Rao, E. V. Sampathkumaran, R. Nagarajan, G. Paul, J. N. Behera and A. Choudhury, *Chem. Mater.*, 2004, **16**, 1441.
- 46 P. Manikandan, K. Padmakumar, K. R. Justin Thomas, B. Varghese, H. Onodera and P. T. Manoharan, *Inorg. Chem.*, 2001, **40**, 6930.
- 47 MAGMUN4.1/OW01.exe is available as a combined package free of charge from the authors (<http://www.ucs.mun.ca/~lthomp/magmun>). MAGMUN has been developed by Dr Zhiqiang Xu (Memorial University), and OW01.exe by Dr O. Waldmann. We do not distribute the source codes. If either routine is used to obtain scientific results, which are published, the origin of the programs should be quoted.
- 48 O. Kahn, *Molecular Magnetism* VCH, New York, 1993.